Part 2 The study of some problems in photonic crystal

Chapter 6

Coupling technique for efficient interfacing between silica waveguides and planar photonic crystal circuits

Yuan-Fong Chau , Tzong-Jer Yang

6.1 Introduction

The photonic crystal (PC) waveguides are expected to play an important role in the development of highly integrated optical circuits (IOCs). Owing to its relevant features such as manufacturing possibilities (Since their planar fabrication allows the use of conventional microelectronics patterning techniques.), compactness and small size, the planar photonic crystal (PPC) technology has attracted great interest to develop microscale IOCs. Refer to[1], the PPC have been designed to simplify manufacturing complexity. It has been predicted and shown that light can be efficiently guided by creating line defects in PPC structures. However, propagation losses arising from coupling integrated dielectric waveguides to PPC waveguides was traditionally high. Thus, it is necessary to develop reliable PPC circuits to minimize the coupling losses between conventional silica waveguides (SWG) and PPC waveguides. Recently, several coupling structures and techniques have been proposed [2-7]. Among all the proposed methods, one of the most promising approaches are PPC tapers[6, 7] mainly due to its small coupling length ($< 5\mu m$) and high coupling efficiencies achieved over a large frequency range with transmission peaks exceeding 80% at localized frequencies, but show some complexity in the procedure to obtain the optimal schemes. However, these structures are very sensitive to manufacturing inaccuracies and as the experimental realization of such structures is much more difficult because of using too many defects and varying the rod sizes to achieve an artificial material with a gradient effective index and an adiabatic mode transformation.   A challenge that must be met if PC waveguides are to be used in IOCs is to find a way to couple light efficiently from SWG into and out of the defects line in photonic band gap (PBG) materials. Because of the different physics of traditional index guiding and PBG guiding, coupling light into and out of photonic crystal waveguides is far from trivial.

There can be substantial reflection and scattering from PC waveguide ends, which adversely affects the outcome of transmission measurements. This is a considerable drawback if one is to efficiently test novel PC devices. To overcome this limitation, one needs an efficient waveguide junction design. A novel coupling technique based on setting a single localized defect within a 0.5μm-long PPC tapered waveguide structure in a triangular lattice of circular dielectric rods in air was proposed in[8], which improves significantly the transmission results using only a conventional (one step size lattice constant) PPC taper[5]. However, the transmission is measured inside the PPC waveguide only reached an average value of 62% and the transmission efficiency decreased as the width of the SWG increased. Note that the transmitted optical power through the PPC waveguide is measured inside the PPC waveguide can not present the actual transmission in the output end of SWG. Besides, the wider PPC tapers are required for efficient mode profile matching to wider dielectric waveguides. In this paper, it is shown that the proposed coupling technique can also be employed with wider PPC tapers but, in this case, a pair of defects at the symmetrical positions in the PPC tapers must be designed for the required PPC taper to maximize the transmission efficiency. The introduction of a single localized defect is investigated as well as their effects on the frequency transmission spectra when both input/output coupling sides of a PPC waveguide are considered. By setting properly the defect mode matching at the interface between the SWG and the PPC waveguide is attained, which improves significantly the transmission efficiency compared with the butt-coupled waveguide, the conventional PPC taper without defect and two step size lattice constant PPC taper without and with defects.

6.2 Structure and coupling techniques

The practical use of SWG and PPC taper for coupling IOCs is limited if there are no good approaches to couple light into them efficiently. It is the aim of this paper to present high efficiency coupling technique between SWG and PPC waveguides in the form of square lattice of dielectric rods surrounded by a homogeneous silica medium. Although there have been reported in the form of triangular ones [6-8]. To the best of our knowledge, coupling into this structure has never been thoroughly investigated. In this paper, we restrict our attention to waveguide junctions for this type of waveguides, as this has been the focus of recent theoretical and experimental investigation [9, 10]. The PPC structure considered here is a two-dimensional (2-D) square array of dielectric rods of lattice constant a surrounded by a homogeneous dielectric medium. Rods have a refractive index value of 3.45, which

corresponds to Silicon (Si) at 1.55µm, and a circular cross section of radius 0.2a. The surrounding medium in the PPC has an index value of 1.45, which corresponds to Silica (SiO2) at 1.55µm. SWG has a dielectric index of 1.45, a width of w, and the surrounding dielectric medium is air. This PPC has a large bandgap for TM (i.e. the electric field is oriented in the axis of the rods)   polarized waves. A lattice constant value of 0.465 µm is chosen because of fixing the transmitted band around 1.55µm. This lattice constant value is equivalent to a/λ =0.3 for λ =1.55µm. Such a value is appropriate for transmission at standard optical communication wavelength. For such lattice constant the PPC substrate has a PBG ranges of wavelength in free space from 1.44µm to 1.68µm for TM polarized waves, calculated by a 2-D plane wave expansion (PWE) method [11]. The PPC waveguide is created along the W1 direction (one row of dielectric rods removed in the (1 0) direction of the photonic crystal). A discrete taper is realized by removing three (W3) and five (W5)rods of the original PPC waveguide to form a two step size lattice constant PPC taper as shown in the zone of dashed line in Fig. 6.1, which combines against a defect rod to form a cavity-like environment.

As described in Ref.[12], adiabatic transmission in PPC waveguide may be achieved if it is guarantee that the operating mode for every different features in the PPC waveguide and PPC taper. Therefore the behavior of them may be predicted by calculation of the independent dispersion diagrams. The dispersion relations for the PPC waveguides shown in Fig. 1 are calculated by the PWE method in the frequency domain for given dielectric configurations. We need to identify a supercell with periodic boundary conditions as the computation domain. The supercell dimension is set (19,1, 1). The choice of nineteen cells in the x direction is essentially a guess. The calculation should be repeated with different size supercells to check for convergence. We determine the TM band structures for three different PPC waveguides (W1,W3 and W5) in order to know their features that are different from those in conventional waveguides. The results are shown in Fig.6. 2. The horizontal axis is the wave vector in the direction of the guide, and the band structures shown in the reduced Brilliouin zone scheme. The modes inside the gap are localized to the row of missing rod. The filled circle (dark gray) line in Fig.6. 2 shows the band structure for the guide in the W1 direction. We find a single guide mode inside the band gap. The electric field of the mode has even symmetry with respect to the mirror plane along the guide axis. The mode itself bears a close resemblance to the fundamental mode of a conventional dielectric waveguide. The open circle lines in Fig.6.2 is made by removing three rows of rods in the W3 direction. There are now three guide modes

inside the gap that can again the classified according to their symmetry with respect to the mirror plane along the guide axis. It is generally true that the number of bands inside the band gap equals the number of rows of rods removed when creating the guide. Analogously, when five rows of rods are removed, we pull up five (the solid lines) guide modes at each k (wave vector) from the dielectric band. The three nearby guide modes A, B and C, which is one of the modes of W1, W3 and W5, respectively, at the arrows indicated shown in Fig.6. 2 are close to each other at the normalized frequency a/λ =0.3. It can be seen in Fig. 2, the three modes A, B and C are merged at point D (k_z=0.4098, $(\omega a)/(2\pi c)$=0.3316). It means that they are coupled at point D, i. e., their eigenmodes propagate at the same wavevector. As stated by Bayindir et al.[13], the coupling length $L = a/(2\Delta k)$, where Δk is the difference between two different wavevectors at a given normalized frequency. This formula shows that Δk strongly depends on normalized frequency, implying that the splitting of large dispersion. Obviously, the value of L is achieved to infinity for coupling the PPC waveguide when Δk approaches to zero which takes place at point D and gives arise to merge of the eigenmodes. In Fig. 6.2, the small value of $\Delta k1$, shows the difference of wavevectors between guide mode B and guide mode C at same normalized frequency of 0.3. It can be seen that the splitting of small dispersion is presented, that implies the two types of waveguides which form the two step size lattice constant PPC taper can couple easily from W5 to W3, but shows some difficulties to couple the light wave into guide mode A (from W3 to W1) due to the larger value of $\Delta k2$ (the difference of wavevectors between guide mode A and guide mode B at same normalized frequency of 0.3). Based on above analysis, it should be noted that we have an opportunity to use an optimum defect configuration as a mode matching trick in the two step size lattice constant PPC taper (which is realized by removing three (W3) and five (W5) rods of the original PPC waveguide) for coupling into the PPC waveguide (by removing one (W1) rod of the original PPC waveguide). Therefore proper mode maybe achieved by setting a defect in the PPC taper when the interfaces between SWG and PPC waveguide are controlled in order to avoid the abrupt change in the reflectivity at input/output of resonant cavities.[14, 15]

The investigated coupling structure consists of a PPC taper with a dielectric defect rod as a defect of a different radius. Mode matching is achieved by choosing the optimum defect parameters within the PPC taper. In this paper a special PPC taper structures is constructed, i.e. a 2.4μm-wide/4a (1.86μm)-long two step size lattice constant PPC taper (where a is the lattice constant) with an optimal radius of defect configuration is introduced in the PPC taper

to couple light both into and out of a finite length (15 rows) PPC waveguide, is shown in Fig.1, in which it may be observed that a SWG guides the input light to the tapered input PPC waveguide passing through the dielectric defect rod. Transmitted optical power through the PPC waveguide is measured using two power monitors placed inside the PPC waveguide at point A and at the output end of SWG at point B, as shown in Fig. 6.1. The defect rod within the PPC taper has a radius r and its position z_{opt} along the z-axis is further optimized to achieve the highest coupling efficiency.
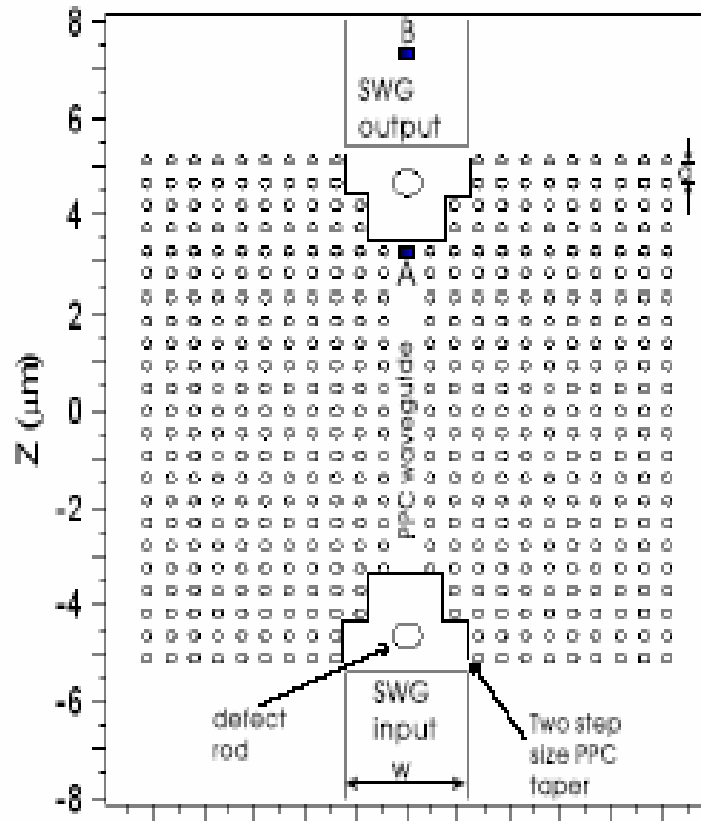

Fig.6.1 Schematic view of the structures considered. A 2.4^{l}m-wide/4a-long two step size lattice constant planar photonic crystal (PPC) taper (Where a is the lattice constant) with a radius of defect configuration is introduced in the PPC taper employed to couple light both into and out of a finite length (15 rows) PPC waveguide from a silica waveguide (SWG). Transmitted optical power through the PPC waveguide is measured using two power monitors placed inside the waveguide at point A and at the output end at point B.
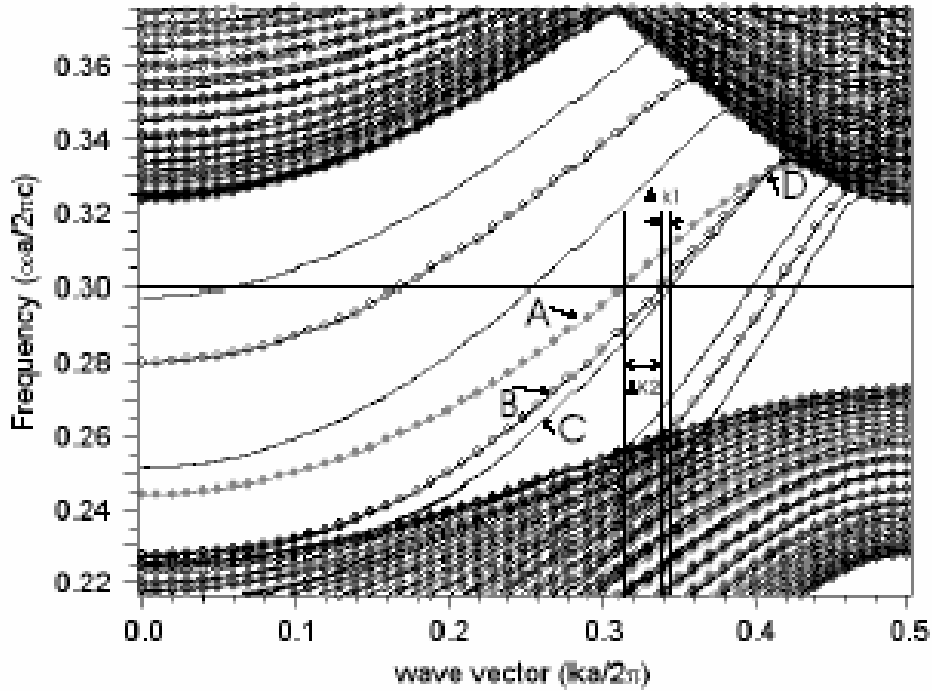
Fig. 6.2. Dispersion relations for the TM band structures for three (W1, W3 and W5) different PPC waveguides in a two-dimensional (2-D) square array of dielectric rods of lattice constant *a* surrounded by a homogeneous dielectric medium. Where W1 (W3, W5) is created by removing one (three, five) rod (rods) of the original PPC waveguide. The three modes A, B and C at the arrows are indicated one of the guide modes of W1, W3 and W5, respectively.

Coupling losses between conventional SWG and PPC waveguides are mainly arising from the mode mismatch derived from the various widths and propagation mechanisms in SWG and PPC waveguides that decreases the coupling efficiency and increases reflection losses. To overcome this issue, the introduction of a single localized defect within the 2.4μm-wide/4*a*- long two step size lattice constant PPC taper alters the modal properties of the guided mode so that mode matching can be achieved by selecting the optimum radius of defect as well as the other optimum parameters (the width of SWG and relative position within the PPC taper). An approach is necessary for setting localized defect into PPC tapers due to the variation of the modal properties along the taper. An optimized study of the proposed coupling technique has been performed by the numerical simulation. This study is aimed to determine the optimum parameter values (the width of SWG *w*, the defect radius *r* and the relative defect position z_{opt} within the two step size lattice constant PPC taper along z

axis at x=0 sectional plane) of the structure shown in Fig. 6.1 in order to achieve the highest coupling efficiency, i.e. maximum transmission through the PPC waveguide from the light coming from input end of SWG to output end of SWG.

6.3 Results and discussions

Let us first optimize the width of SWG and the radius of defect, and further the transmission is improved by optimizing the relative position of the defect that should be placed into the PPC taper. The latter computational method used is based on a 2-D finite difference time domain (FDTD) algorithm [16]. A grid size of $a/50$ is used in the FDTD simulations and the condition of perfectly matched layer (PML) is considered at boundary zone to ensure no back reflection in the limit of the analyzed region [17] which is terminated by 0.5μm width to realize perfectly absorbing boundary conditions. First, the SWG width (w) and the defect position (z_{opt}) and the radius of defect (r) have been optimized at the 0.3 (a/λ) normalized frequency located closed to 1.55 μm for the lattice value considered. In order to excite the modeling structure of the input end of SWG, a sinusoidal monochromatic continuous wave with normalized power has been used as light source in the z-direction with a Gaussian transverse field pattern in the x-direction. Removing several additional dielectric rows as displayed in the upper part of Fig. 6.3 creates different shapes of the PPC taper. Fig. 6.3 shows the normalized transmission spectra of a 15 rows PPC waveguide coupled to an input and output SWG against $w=a$ for four cases: (1) the butt-couple case (the dotted line), (2) the conventional PPC taper (the dashed-dotted line) without defect, (3) the two step size lattice constant PPC taper without defect (the dashed line) and (4) with defect (the solid line) (where defect radius of r=0.3 μm, defect positions are located at (0,-9.7a),(0,+9.7a), respectively. The transmitted field is picked up by a power monitor at point B covering the exit of the PPC waveguide as shown in the Fig.6. 1. The transmission spectra is calculated from the Fourier-transformed time series and normalized with respect to the launched source.

The transmission in the butt-couple case is very low and a maximum transmission of only 47% is achieved when the SWG width is 1.34a. It is clearly that the transmission decreased with the width of SWG increased. For the case of the conventional PPC taper without defect, the transmission is increased with the width of SWG increased and the steady value up to 50% is achieved when the width of SWG more than $6a$ (2.79μ m) . Furthermore,
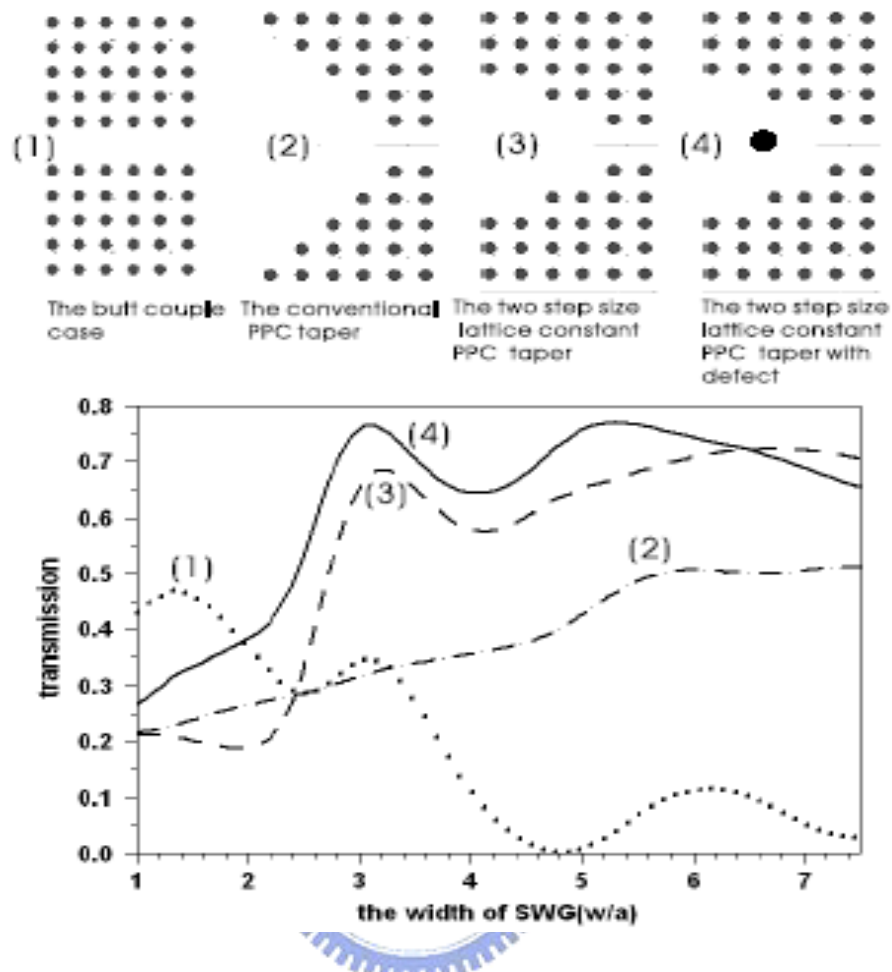
Fig. 6.3. The normalized transmission spectra of a 15 rows PPC waveguide coupled to an input and output SWG against *w/a* for four cases(measured at point B): (1) the butt-couple case (the dotted line), (2) the conventional PPC taper (the dashed-dotted line), (3)the two step size lattice constant PPC taper without defect (the dashed line) and (4) with defect (the solid line) (where defect radius of r=0.3 μm, defect positions are located at (0,-9.7a),(0,+9.7a), respectively. The transmitted field is picked up by a power monitor at point B covering the exit of the PPC waveguide shown in the Fig. 6.1.

the transmission sharply increases when the two step size lattice constant PPC taper without defect is used, achieving a transmission up to 57% for a SWG width more than 3.2*a* (1.49μm). Nevertheless, the introduction of a defect within the two step size lattice constant PPC taper improves the transmission up to 64% for a SWG width ranging above 3.1*a* (1.44μm). It should be noted that the transmission spectra obtained in case (3) and (4) are very similar, which indicates that the defect only acts as a mode impedance matching technique improving

the transmission but without modifying the spectral. The optimum SWG widths to achieve the maximum transmission (78%) are $3.17a$ (1.5μm) and $5.22a$ (2.4μm). For case (4), for which the SWG width is increased the transmission counterintuitively decrease than case (3) for SWG width above 6.512a (3.03¹m). Therefore, configuration (4) seems to be a local optimum when the SWG width is ranging from 3.1a to 6.512a. One of the reasons is that as the SWG width increases above 6.512a, in the case of coupling into the PPC waveguide has a lower efficiency, because in this case there are many channels into which a wave reflected from the junction can couple.

Fig. 6.4 shows the transmission spectra against the defect radius (r) normalized to the lattice constant (a) of the PPC, for the case using the optimum SWG width (w_{opt}=2.4μm) obtained previously. Transmitted optical power through the PPC waveguide is measured
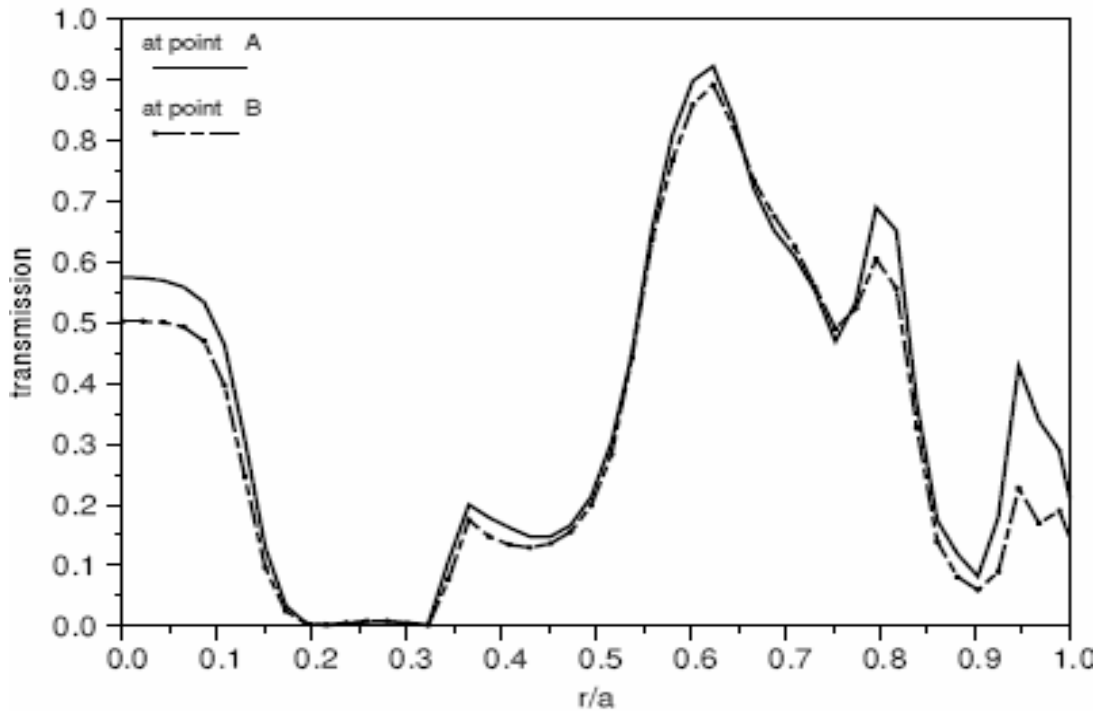

Fig. 6.4. The transmission spectra against the defect radius r normalized to the lattice constant *a* of the PPC, for the case using the optimum SWG width (w_{opt}=2.4μm) obtained previously. Transmitted optical power through the PPC waveguide is measured using two power monitors located at point A and B, respectively.

using two power monitors located at point A and B, respectively, as shown in Fig. 6.1. In Fig. 6.4 it can be seen that the maximum transmission (93% at point A, 90% at point B), is achieved for r=0.622a (0.289 μm) instead of r=0.3μm, which is considered in previous simulations, that confirms the assumption made to obtain the results shown in Fig.6. 3. It should be emphasized that the transmission spectra measured at points A and B using PPC tapered waveguides at SWG output end are very similar, which indicates that the defect at output end only acts as a mode impedance matching technique improving the transmission but without modifying the spectra. In addition, when the light wave propagates along the output end of PPC waveguide, as it traverses the defect in the PPC taper of output end, some of it is reflected, and some of it is lost to the radiation modes in the vacuum. The rest is mostly propagates into the output end of SWG. It can be observed in Fig. 6.4 that the maximum transmission shown the 3% difference measured at point B and point A, that is to say the coupling lost is merely 3% which confirms the introduction of localized defects within the two step size lattice constant PPC taper structure can hold the transmitted light efficiently emerging from the PPC waveguide along the z-axis (shown in Fig. 6.1), and is satisfied resulting in a mode match that increases the coupling efficiency and decreases reflection losses. By the way, if the size of defect radius is controlled properly in the range of 0.2a to 0.33a within input and output PPC taper, the PPC circuit can be used as a good reflector.

The optimum relative position of the defect along both x-axis and z-axis has also been investigated. Based on our simulations, variations in the x-axis indicates that the optimum position is x=0 (see in Fig.6.1), which corresponds to the mirror symmetry axis. Regarding the position along z-axis, the normalized transmitted power obtained as a function of z/a at points A and B for the case of coupling with two sides of the PPC waveguide with the 2.4μm-wide 4a-long two step size lattice constant PPC taper to the SWG and for a fixed normalized frequency of 0.3(a/λ) is shown in Fig. 6.5. It can be seen that there is one z/a position that provides relative transmission maximums: $z_{opt} = 10.4a$. By setting single defect at single position depicted in Fig.6.5. It should also be indicated that the transmission is above 80% for a range of the defect position z from 0.981a to 10.57a. Namely, it can provide a large range of tolerance of the defect position for manufacturing inaccuracies.

Fig. 6.4 depicts the normalized transmitted power as a function of the defect radius r normalized to the lattice constant of a for single defect regarding the PPC tapered waveguide. The optimization procedure employed will be briefly described as follows. After fixing the
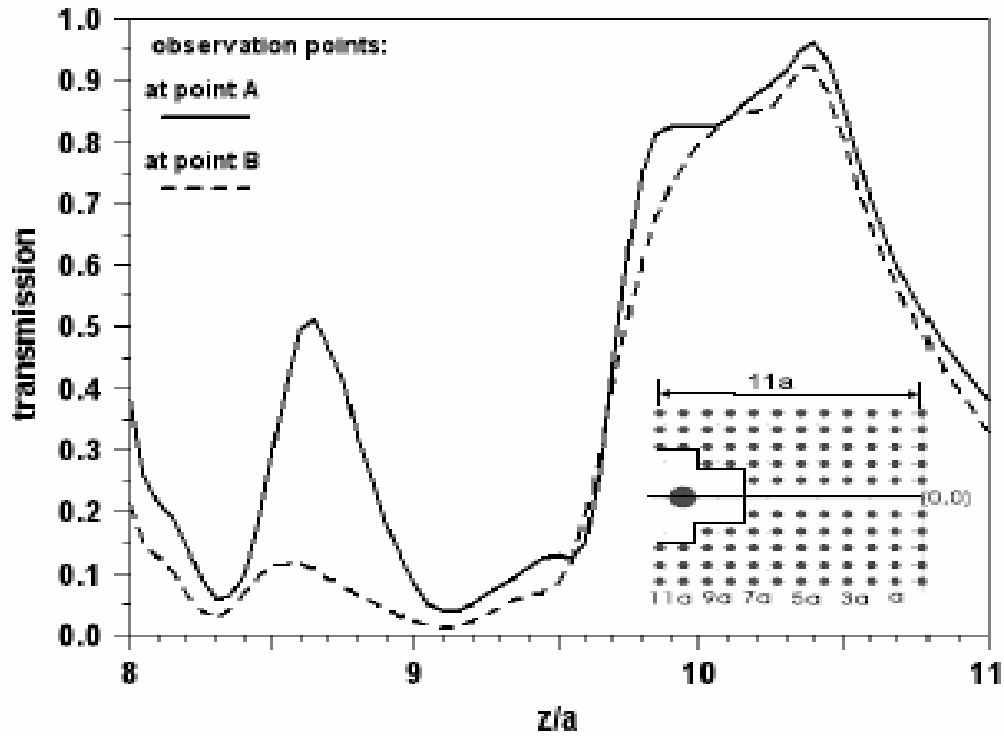
Fig. 6.5. The normalized transmitted power obtained as a function of z/a at point A and B for the case of coupling with two side of the PPC waveguide with the 2.4μm-wide 4*a*-long two step size lattice constant PPC taper to the SWG and for a fixed normalized frequency of 0.3(a/λ).

single defect with radius r at the optimum $z=a$ positions shown in Fig. 6.5. Then setting the single defect within the PPC taper at the optimum positions and with the optimum radius the peak transmission at 0.3(a/λ), which corresponds to a wavelength of 1.55μm for the lattice constant value of 0.465μm, is enhanced above 90% (measured at point B shown in Fig.6.1.) transmission from a nearly 40% transmission when a conventional (one step size lattice constant) PPC taper structure without defect is considered. Figure 6.6(a) and 6.6(b) shows the steady state of the electric field (E_y) for the input/output coupling employing the 2.4μm wide 4*a*-long conventional PPC taper without defect and two step size lattice constant PPC taper with the optimized single-defect configuration both input and output ends obtained previously, respectively. Based on our simulations, we find the aspect of PPC taper structure can be acted as a key factor for coupling efficiency between conventional SWG and PPC taper, i.e. the two step size lattice constant aspect is superior to the other forms of PPC taper in the coupling

process, especially in the form of 2-D square lattice of dielectric rods in the silica medium structure. The conventional PPC taper without defect shown in Fig. 6.6(a) appears a standing-wave pattern in the input SWG. The coupling losses is reflected from junctions between the input end of SWG and PPC taper, some propagates back to the input end of SWG, and some decays by the sides of input end of   SWG. It has a sinusoidal profile inside the PPC waveguide. When the light wave emerges from the output end of PPC taper, some propagates inside the output end of SWG and some decays exponentially in air. It is clearly that the field pattern in the output end of PPC taper in Fig6.6(a) is obviously weaker than that exists in the input end. Conversely, the field pattern inside the input end of PPC taper is nearly the same as that appears in output end shown in Fig.6.6(b). This confirm that the suitable PPC tapered structure with an optimum defect rod will perform a key factor which increases the coupling efficiency and decreases the reflection losses. The PPC taper provide a surrounding to form the suitable field pattern that the defect rod can efficiently hold the light wave and form a new center of light source in the cavity-like structure in the PPC taper. Therefore, a better coupling from the SWG through the PPC taper to the PPC waveguide is achieved when the optimum defect configuration is employed shown in Fig 6. 6 (b). Note that the constructive interference exists in the input/output PPC tapers which enhances the coupling efficiency are mainly caused due to the use of the optimum defect configuration.
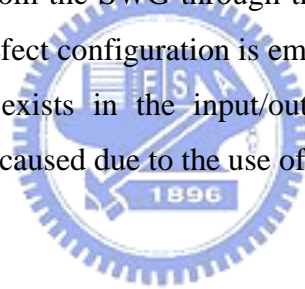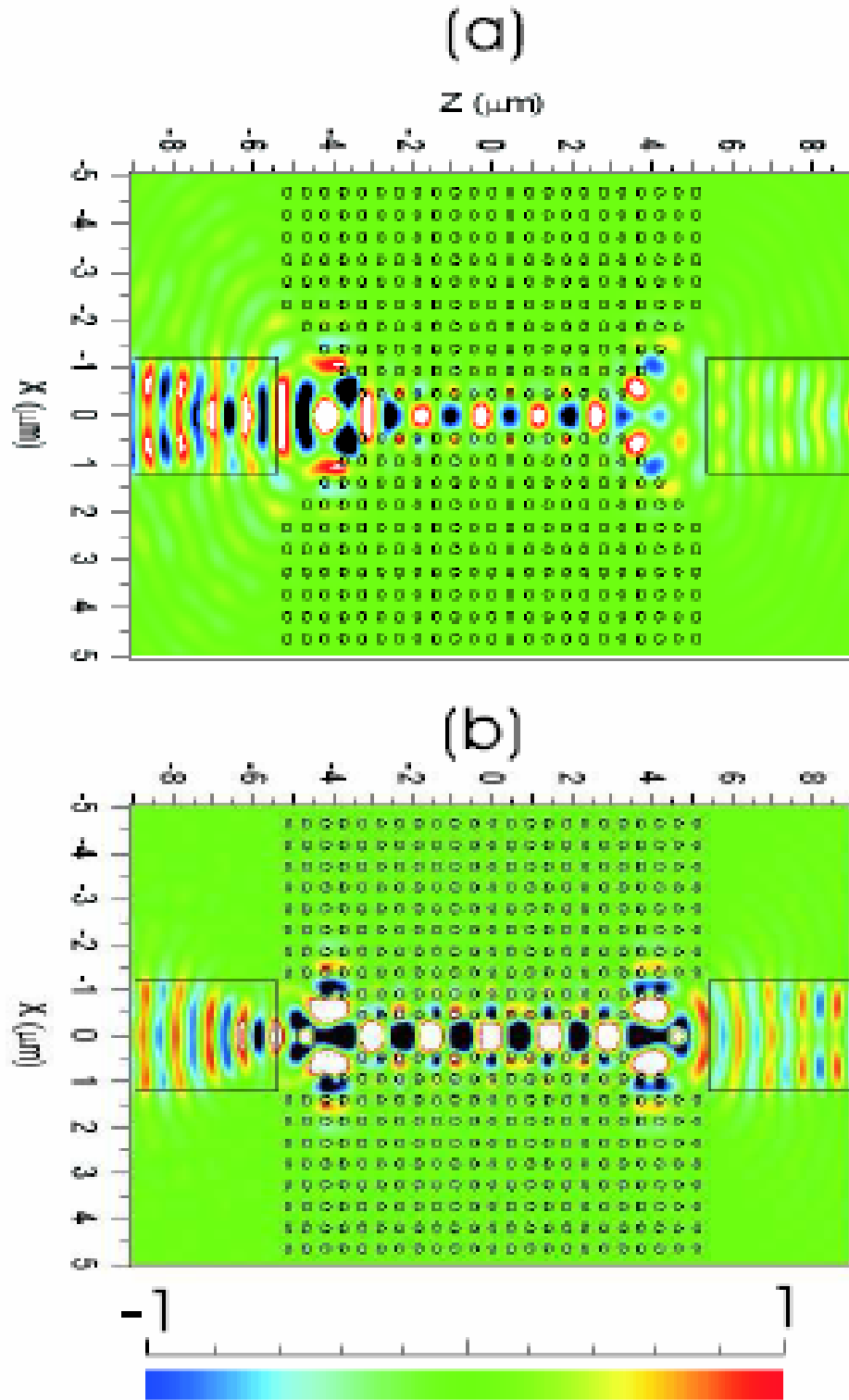
Fig. 6.6. The steady state of the electric field for the input=output coupling employ the 2.4μm wide 4a-long PPC taper: (a) the conventional PPC taper without defect and (b) two step size lattice constant PPC taper with the optimized single-defect configuration both input and output ends obtained previously.

Fig.6.7 shows the normalized transmission spectra of a 15 rows PPC waveguide coupled to an input and output SWG against a/λ, for five cases: (1) 0.5μm width two step size lattice constant PPC taper with defect (a/λ=0.3, the dotted line), (2) 2.4μm width two step size lattice constant PPC taper without defect (a/λ=0.3, the solid line), (3) the same as case (2) except with defect (solid-dotted line), (4) the same as case (3) except a/λ=0.289 (dashed line), and (5) the same as case (3) except a/λ=0.306 (dashed-dotted line). To obtain these results, an incident pulsed field was launched at the input end of SWG. The fundamental mode of SWG is excited by a pulsed wave that propagates along the z-direction and the transmission spectra field is calculated with the overlap integral between the launched and measured field shown in the Fig.6. 1. The transmission spectra is calculated from the Fourier-transformed time series and normalized with respect to the launched pulse. The transmission spectra against the normalized frequency for a 15-ro w-long PPC waveguide coupled to both an input and output SWG with a 4a-long PPC taper using the single-defect configuration (see Fig.6.1) and without defect is depicted in Fig. 6.7. The lower transmission is presented in case (1) due to the narrower width of SWG that is agreement with the results of case (4) shown in Fig. 6.3. The resonances that appears in the transmission spectrum of the PPC taper without defect in case (2) are due to the Bragg reflection created by the mode mismatching at the interfaces between the SWG and PPC taper and thus the number of resonances dependents on the length of PPC taper. When the proposed defect configuration is set the response sharply diminish because a better mode matching at the interfaces of the PPC waveguide is achieved. According to the case (3) in Fig. 6.7, an average transmission level larger than of 80% is achieved for a normalized frequency range from 0.294(a/λ) to 0.302(a/λ) and the maximum transmission above 90%, which enhances the 26.9% average transmission level achieved with the PPC taper without defects when the SWG width was 2.4μm. However, in Fig. 6.7 it can be observed that the bandwidth of case (3) is smaller although it still satisfies bandwidth requirements for optical communications. One of the reasons for this is that the defect is used to achieve high coupling efficiency. That is to say, the high coupling efficiency is achieved at the sacrifice of bandwidth which becomes more sensitive to the normalized frequency employed to optimize the parameters of the defects. In order to illustrate this point the same optimization procedure was employed but for two different normalized frequencies of 0.289(a/λ) and 0.306(a/λ) shown in the case (4) and case (5) in Fig. 6.7. In case (5) of the normalized frequency of 0.306(a/λ), the optimum single-defect configuration was obtained

for r_{opt} = 0.3μm and z_{opt} = 10a. It can be seen that the case (3), (4) and (5) in Fig. 6.7, the transmission spectra is shifted towards the normalized frequency employed in the optimization procedure. This means that the central frequency will be controlled for optical communications by means of determining the optimal parameters in defect configuration in PPC tapers.
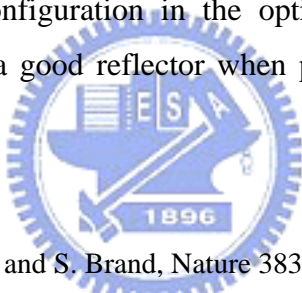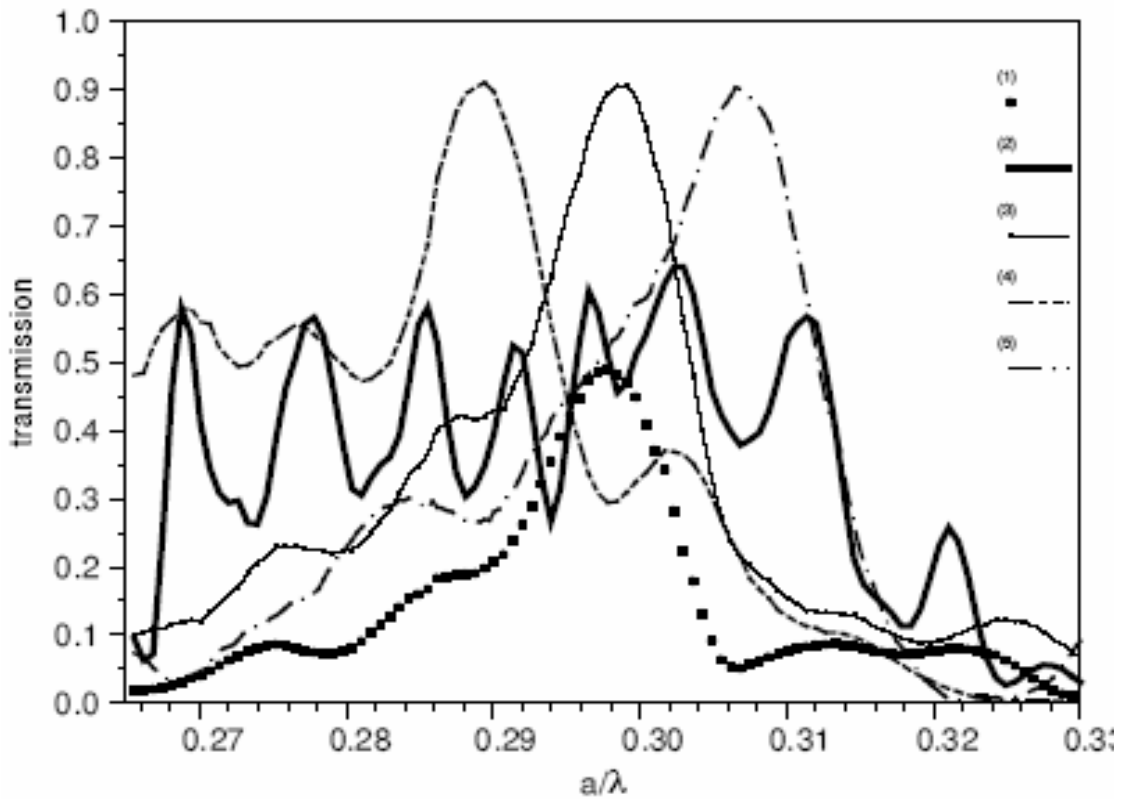

Fig. 6.7 The normalized transmission spectra of a 15 rows PPC waveguide coupled to an input and output SWG against a/λ for five cases: (1) 0.5μm width two step size lattice constant PPC taper with defect (a/λ=0.3, the dotted line), (2) 2.4μm width two step size lattice constant PPC taper without defect(a/λ=0.3, the solid line), (3) the same as case (2) except with defect (solid-dotted line), (4) the same as case (3) except a/λ=0.289 (dashed line), and (5) the same as case (3) except a/λ=0.306 (dashed-dotted line).

6.4 Summary

In conclusion, we report a coupling technique based on setting single localized defect within a PPC tapered waveguide in the form of a 2-D square lattice of dielectric rod in the silica medium structure. The coupling technique achieves mode matching at the interface of input and output between SWG and PPC waveguides reducing reflection losses and improving significantly the transmission efficiency. An optimization procedure to choose the optimum parameters of defect as well as waveguide parameters have been optimized to achieve highest transmission. The simulation results show that by setting properly single defect within a 2.4μm-wide/4a-long two step size lattice constant PPC taper a transmission above 90% at a standard optical communication wavelength of 1.55μm can be achieved, which sharply enhances the transmission obtained when no defects are considered. It is robust against manufacturing inaccuracies and is valid for both coupling into and out of a photonic crystal waveguide. Finally, it is worth mentioning that the central frequency can be controlled by determining this defect configuration in the optimization procedure. In addition, the proposed structure can act as a good reflector when properly adjusting the range of defect radius.

References

[1] T. F. Krauss, R. M. De La Rue and S. Brand, Nature 383, 699-702 (1996).

[2] M.E. Potter and R.W. Ziolkowski, Opt. Express, 10 691, (2002).

[3] Y. Xu, R. Lee, and A. Yariv, Opt. Lett. 25, 755-757 (2000).

[4] A. Mekis and J.D. Joannopoulos, IEEE J. Lightwave Technol. 19, 861-865 (2001).

[5] T.D. Happ, M. Kamp and A. Forchel, Opt. Lett. 26,1102-1104 (2001).

[6] P. Sanchis, J. Marti, J. Blasco , A. Martinez and A Garcia, Opt. Express 10, 1391 (2002).

[7] Jianhua Jiang, Jingbo Cai, Gregory P. Nordin, and Lixia Li, Opt. Lett. 28, 2381(2003).

[8] P. Sanchis, J. Marti, A. Garcia, A. Martinez and J. Blasco, Electron. Lett. 38, 961-962 (2002).

[9] A. Mekis, J. C. Chen, I. Kurland, S. Fan, P. R. Villeneuve, and J. D. Joannopoulos, Phys. Rev. Lett., vol. 77, pp. 3787-3790, (1996).

[10] S.-Y. Lin, E. Chow, V. Hietala, P. R. Villeneuve, and J. D. Joannopoulos, Science, vol. 282, pp. 274-276, (1998).

[11] See http://ab-initio.mit.ed/mpb.

[12] S. G. Johnson and J. D. Joannopoulos, Opt. Express 8, 173 (2001).

[13] M. Bayindir, B. Temelkuran, and E. Ozbay, Phys. Rev. Lett. 84, 2140 (2000).

[14] T. J. Karle, D. H. Brown, R. Wilson, M. Steer, and T. E. Karuss, IEEE J. Sel. Top. Quantum Electron, 8, 909(2002).

[15] Y. Xu, R. Lee, and A. Yariv, Opt. Lett. 25, 755(2000).

[16] A. Taflove, Computational Electrodynamics (Artech, Norwood, MA, 1995).

[17] J. P. Berenger, J. Comput. Phys. 114,185-200 (1994).